DOI 10.1002/pmic.200402070 *Proteomics* 2006, *6,* 1518–1529

RESEARCH ARTICLE

Reconstruction of central carbon metabolism in *Sulfolobus solfataricus* using a two-dimensional gel electrophoresis map, stable isotope labelling and DNA microarray analysis

Ambrosius P. L. Snijders[1], Jasper Walther[2]*, Stefan Peter[1], Iris Kinnman[1], Marjon G. J. de Vos[1, 2], Harmen J. G. van de Werken[2], Stan J. J. Brouns[2], John van der Oost[2] and Phillip C. Wright[1]*

[1] Biological and Environmental Systems Group, Department of Chemical and Process Engineering, University of Sheffield, Sheffield, UK
[2] Laboratory of Microbiology, Department of Agrotechnology and Food Sciences, Wageningen University, Wageningen, The Netherlands

In the last decade, an increasing number of sequenced archaeal genomes have become available, opening up the possibility for functional genomic analyses. Here, we reconstructed the central carbon metabolism in the hyperthermophilic crenarchaeon *Sulfolobus solfataricus* (glycolysis, gluconeogenesis and tricarboxylic acid cycle) on the basis of genomic, proteomic, transcriptomic and biochemical data. A 2-DE reference map of *S. solfataricus* grown on glucose, consisting of 325 unique ORFs in 255 protein spots, was created to facilitate this study. The map was then used for a differential expression study based on ^{15}N metabolic labelling (yeast extract + tryptone-grown cells (YT) *vs.* glucose-grown cells (G)). In addition, the expression ratio of the genes involved in carbon metabolism was studied using DNA microarrays. Surprisingly, only 3 and 14% of the genes and proteins, respectively, involved in central carbon metabolism showed a greater than two-fold change in expression level. All results are discussed in the light of the current understanding of central carbon metabolism in *S. solfataricus* and will help to obtain a system-wide understanding of this organism.

Received: December 17, 2004
Revised: August 12, 2005
Accepted: August 22, 2005

Keywords:
Archaea / DNA microarray / Glycolysis / Mass spectrometry / Metabolic labelling

Correspondence: Professor Phillip C. Wright, Biological and Environmental Systems Group, Department of Chemical and Process Engineering, University of Sheffield, Mappin Street, Sheffield S1 3JD, UK
E-mail: p.c.wright@sheffield.ac.uk
Fax: +44-114-222-7501

Abbreviations: ED, Entner–Doudoroff pathway; **EMP**, Embden–Meyerhof–Parnas pathway; **GAP**, glyceraldehyde-3-phosphate; **GAPN**, nonphosphorylating GAP dehydrogenase; **KDG**, 2-keto-3-deoxy-gluconate; **MOWSE**, molecular weight search; **PK**, pyruvate kinase; **PPP**, pentose phosphate pathway; **TCA**, tricarboxylic acid cycle

1 Introduction

Sulfolobus solfataricus is a thermoacidophilic crenarchaeon, which grows between 70 and 90°C and in a pH range of 2–4 [1]. Its preference for environments hostile to many other organisms makes it an interesting source for novel, thermostable enzymes. *S. solfataricus* has been an attractive crenarchaeal model organism since its isolation in the early 1980s, and the completion of the genomic sequence in 2001

* Both authors contributed equally to this work

[2] has further increased its popularity. Currently, 1941 genes (53.11%) in TIGR's comprehensive microbial resource (CMR) database have no known function [3]. Of the 2977 ORFs originally identified in the genome of *S. solfataricus*, 40% of the genes are archaea specific, 12% are bacteria specific and 2.3% are shared exclusively with eukaryotes. Currently, genetic tools are under development, which will contribute to our understanding of fundamental processes in *Sulfolobus* [4–8]. In order to fully exploit its potential for metabolic engineering, a deeper understanding of the central energy and precursor generating pathways is necessary.

The central metabolic pathways in archaea contain many unique features compared to the classical pathways in bacteria and eukaryotes [9, 10]. In *S. solfataricus*, glucose degradation proceeds *via* a nonphosphorylated version of the Entner–Doudoroff (ED) pathway [11–13]. In this pathway, glucose is converted into pyruvate through the action of glucose dehydrogenase, gluconate dehydratase, 2-keto-3-deoxy-gluconate (KDG) aldolase, glyceraldehyde dehydrogenase, glycerate kinase, enolase and pyruvate kinase (PK). Recently, experimental evidence has been provided for the operation of the semiphosphorylated ED pathway in *S. solfataricus* in which KDG is phosphorylated [14]. Gluconeogenesis *via* a reversed ED pathway is unlikely, since the key enzymes in this pathway do not seem to be able to distinguish between glucose and galactose derivatives. In this case, gluconeogenesis *via* a reversed ED pathway would result in a mixture of glucose and galactose [15]. Instead, *in silico* analysis of the *Sulfolobus* genomes as well as experimental evidence has revealed the presence of a near complete set of proteins involved in the Embden–Meyerhof–Parnas (EMP) pathway [9], suggested to be active in the gluconeogenic direction rather than in the glycolytic direction [16].

In this study, we reconstructed central carbon metabolism and the tricarboxylic acid cycle (TCA) cycle on the basis of biochemical, computational, proteomic and DNA microarray data, obtained from cell extracts of *S. solfataricus* grown on sugars and peptides. First of all, a 2-DE map was created to provide a global overview of protein expression under glucose-degrading conditions. This map was then used to investigate the relative abundance of proteins involved in sugar metabolism under minimal or rich media through a ^{15}N metabolic labelling approach. Moreover, DNA microarray analysis was performed to compare mRNA expression under the same conditions. In the last few years, similar transcriptome studies have been conducted with several archaea that utilise different types of glycolysis. These organisms include: *Pyrococcus furiosus* [17], an obligate anaerobic hyperthermophile with an EMP-like pathway and *Haloferax volcanii* [18] a facultative anaerobic halophile using an ED-like glycolysis. However, there are relatively few studies that combine transcriptomics and proteomics, and none have so far been published for archaea.

Here, we present a study in which both quantitative proteomics and transcriptomics were used to analyse the expression of the genes involved in the central carbon metabolism of *S. solfataricus*.

2 Materials and methods

2.1 Cell growth and harvest

S. solfataricus P2 (DSM1617) was grown aerobically in a rotary shaker at 80°C in a medium of pH 3.5–4.0 which contained: 2.5 g/L $(NH_4)_2SO_4$, 3.1 g/L KH_2PO_4, 203.3 mg/L $MgCl_2 \cdot 6H_2O$, 70.8 mg/L $Ca(NO_3)_2 \cdot 4H_2O$, 2 mg/L $FeSO_4 \cdot 7H_2O$, 1.8 mg/L $MnCl_2 \cdot 4H_2O$, 4.5 mg/L $Na_2B_4O_7 \cdot 2H_2O$, 0.22 mg/L $ZnSO_4 \cdot 7H_2O$, 0.06 mg/L $CuCl_2 \cdot 2H_2O$, 0.03 mg/L $Na_2MoO_4 \cdot 2H_2O$, 0.03 mg/L $VOSO_4 \cdot 2H_2O$ and 0.01 mg/L $CoCl_2 \cdot 6H_2O$. The medium was supplemented with Wollin vitamins, and either 0.3–0.4% D-glucose (G) or 0.1% yeast extract and 0.2% tryptone (YT). The Wollin vitamin stock (100×) contained 2 mg/L D-biotin, 2 mg/L folic acid, 10 mg/L pyridoxine-HCl, 10 mg/L riboflavin, 5 mg/L thiamine-HCl, 5 mg/L nicotinic acid, 5 mg/L DL-Ca-pantothenate, 0.1 mg/L vitamin B12, 5 mg/L *p*-aminobenzoic acid and 5 mg/L lipoic acid. Cell growth was monitored by measuring the turbidity at 530 or 600 nm. Cells for the proteome reference map were harvested by centrifugation in the late-exponential growth phase at an OD_{530} of 1.0. Cells were washed twice with a 10 mM Tris/HCl buffer (pH = 7). Subsequently, cells were stored at −20°C until required. During this whole process, considerable care was taken to ensure that culture to culture variation was minimised, and cultures were prepared in at least triplicate. In the case of the ^{15}N labelling experiment, $(^{15}NH_4)_2SO_4$ was used as the nitrogen source. Cells were incubated with ^{15}N ammonium sulphate for at least eight doubling times to allow full incorporation of the label. After this, the ^{14}N and ^{15}N growth experiments were set up simultaneously. When OD reached a value of 0.5, the cultures were mixed. To ensure that equal amounts of biomass were mixed, slight corrections in volume were made in case the OD_{530} was not exactly 0.5. Previously, we have demonstrated that this approach leads to accurate mixing [19]. Next, cells were pelleted by centrifugation, washed twice with a 10 mM Tris/HCl buffer (pH = 7) and stored at −20°C. Preparation of cell extracts, 2-DE and protein identification were performed in exactly the same manner for the labelled/unlabelled cells as for the unlabelled cells.

2.2 Preparation of cell extracts

The −20°C frozen cells were thawed and immediately resuspended in 1.5 mL of 10 mM Tris/HCl buffer (pH = 7), and 25 μL of a protease-inhibitor cocktail (Sigma) was added. Cells were disrupted by sonication for 10 min on ice ("Soniprep 150", Sanyo). Insoluble cell material was removed by centrifugation at 13 000 rpm for 10 min. The protein concentration of the supernatant was determined using the Bradford Protein Assay (Sigma). The supernatant was subsequently stored at −80°C.

2.3 2-DE

Gels for the reference map were prepared in triplicate. The extract was mixed with a rehydration buffer containing 50 mM DTT (Sigma), 8 M urea (Sigma), 2% CHAPS (Sigma), 0.2% w/v Pharmalyte ampholytes pH 3–10 (Fluka) and bromophenol blue (trace) (Sigma). This mixture was designated as the sample mix. Three IPG strips (pH 3–10) (BioRad) were rehydrated with 300 μL (400 μg) of this sample mix. Strips were allowed to rehydrate overnight. IEF was performed using a three-step protocol at a temperature of 20°C using a Protean IEF cell (BioRad). In the first step, the voltage was linearly ramped to 250 V over 30 min to desalt the strips. Next, the voltage was linearly ramped to 10 000 V over 2.5 half-hour periods. Finally, the voltage was rapidly ramped to 10 000 V for 40 000 V/h to complete the focussing. At this stage, the strips were stored overnight at −20°C. Focussed strips were first incubated for 15 min in a solution containing 6 M urea, 2% SDS, 0.375 M Tris-HCl (pH 8.8), 20% glycerol and 2% w/v DTT. After this, the solution was discarded and the strips were incubated in a solution containing 6 M urea, 2% SDS, 0.375 M Tris-HCl (pH 8.8), 20% glycerol and 4% iodoacetamide. After equilibration, proteins were separated in the second dimension by SDS-PAGE performed using a Protean II Multicell (BioRad) apparatus on 10% T, 2.6% C gels (17 cm × 17 cm × 1 mm). Electrophoresis was carried out with a constant current of 16 mA/gel for 30 min; subsequently the current was increased to 24 mA/gel for another 7 h.

2.4 Protein visualization and image analysis

Gels were stained using CBB G-250 (Sigma). Gels were scanned using a GS-800 densitometer (BioRad) at 100 μm resolution. All spot detection and quantification was performed with PDQUEST 7.1.0 (BioRad). Staining intensity was normalised against the total staining intensity on the gel. Two hundred fifty-five spots were selected for mass spectrometric analysis. For protein quantitation, metabolic labelling was used, and for this gel image was matched to the reference map and protein spots of interest were selected for MS analysis and quantitation.

2.5 Protein isolation and identification by MS

Spots of interest were excised from the stained 2-DE gels by hand, destained with 200 mM ammonium bicarbonate with 40% ACN. The gel pieces were incubated overnight in a 0.4 μg trypsin solution (Sigma) and 50 μL of 40 mM ammonium bicarbonate in 9% ACN. The next day, peptides were extracted in three subsequent extraction steps using 5 μL of 25 mM NH_4HCO_3 (10 min, room temperature), 30 μL ACN (15 min, 37°C), 50 μL of 5% formic acid (15 min, 37°C) and finally with 30 μL ACN (15 min, 37°C). All extracts were pooled and dried in a vacuum centrifuge, then stored at −20°C.

The lyophilised peptide mixture was resuspended in 0.1% formic acid in 3% ACN. This mixture was separated on a PepMap C-18 RP capillary column (LC Packings, Amsterdam, The Netherlands) and eluted in a 30-min gradient *via* an LC Packings Ultimate nanoLC directly onto the mass spectrometer. Peptides were analysed using an Applied Biosystems QStarXL® ESI quadrupole TOF tandem mass spectrometer (ESI qQ-TOF). The data acquisition on the MS was performed in the positive ion mode using information dependent acquisition (IDA). Peptides with charge states 2 and 3 were selected for MS/MS. IDA data were submitted to MASCOT for database searching in a sequence query type of search (www.matrixscience.com). The peptide tolerance was set to 2.0 Da and the MS/MS tolerance was set to 0.8 Da. A carbamidomethyl modification of cysteine was set as a fixed modification and methionine oxidation was set as a variable modification. Up to one missed cleavage site by trypsin was allowed. The search was performed against the MS protein sequence database (MSDB; ftp://ftp.ncbi.nih.gov/repository/MSDB/msdb.nam). Molecular weight search (MOWSE) [20] scores greater than 50 were regarded as significant.

2.6 Peptide quantitation

In the metabolic labelling experiments, peptide identification of the light (^{14}N) version of the peptide was performed as described in Section 2.5. After this, the heavy ^{15}N version of the peptide could be identified by changing the isotope abundance of ^{15}N nitrogen to 100% in the Analyst software data dictionary. Next, the peak area of both versions of the same peptide was integrated over time using LC-MS reconstruction tool in the Analyst software. In addition, an extracted ion chromatogram (XIC) was constructed for each peptide. The XIC is an ion chromatogram, which shows the intensity values of a single mass (peptide) over a range of scans. This tool was used to check for chromatographic shifts between heavy and light versions of the same peptide.

2.7 RNA extraction and probe synthesis

Early-log phase cultures (OD_{600} 0.1–0.2) of *S. solfataricus* grown on 0.1% yeast extract and 0.2% tryptone (YT) or 0.3% D-glucose (G) were quickly cooled in ice-water and harvested by centrifugation at 4°C. The RNA extraction was done as described previously [21]. Preparation of cDNA was done as follows: to 15 μg of RNA, 5 μg of random hexamers (Qiagen) was added in a total volume of 11.6 μL. This was incubated for 10 min at 72°C after which the mixture was cooled on ice. Next, dATP, dGTP and dCTP (5 μM final concentration) were added, together with 4 μM aminoallyl dUTP (Sigma), 1 μM dTTP, 10 mM DTT, 400 U superscript II (Invitrogen) and the corresponding 5 × RT buffer in a final volume of 20 μL. The reverse transcriptase reaction was carried out at 42°C for 1 h. To stop the reaction and to degrade the RNA, 2 μL 200 mM EDTA and 3 μL 1 M NaOH were added to the reaction mixture, after which it was incubated at

70°C for 15 min. After neutralisation by the addition of 3 μL 1 M HCl, the cDNA was purified using a Qiagen MinElute kit according to the manufacturer, except that the wash buffer was replaced with 80% v/v ethanol. The cDNA was then labelled using postlabelling reactive CyDye packs (Amersham Biosciences), according to the protocol provided by the company. Differentially labelled cDNA derived from *S. solfataricus* cells grown on either YT or G media was pooled (15 μg labelled cDNA of each sample) and excess label was removed by cDNA purification using the MinElute kit.

2.8 DNA microarray hybridisation, scanning and data analysis

The design and construction of the microarray, as well as the hybridisation was performed as described previously [22, 23]. After hybridisation, the microarrays were scanned at a resolution of 5 μm with a Genepix 4000B scanner (Axon Instruments) using the appropriate laser and filter settings. Spots were analysed with the Genepix pro 5.0 software package (Axon Instruments). Low-quality spots were excluded using criteria that were previously described [22]. ^{2}Log-transformed ratios (^{2}log(YT/G)) from the replicate slides were averaged after first averaging the duplicate spots on the array. Statistical significance for the observed ratios was calculated by doing a significance analysis of microarrays (SAM) analysis [24]. Each ^{2}log value represents two hybridisation experiments, performed in duplicate by using cDNA derived from four different cultures of *S. solfataricus*: two grown on YT media and two grown on glucose media. The result of each ORF therefore consisted of eight pairwise comparisons. The ORFs were categorised according to the 20 functional categories of the CMR [3].

2.9 Metabolic pathway reconstruction based on biochemical and genomic data

The reconstruction of the main metabolic pathways was performed with BLASTP and PSI-BLAST programmes [25] on the nonredundant (NR) database of protein sequences (National Center for Biotechnology Information) by using full length or N-terminal protein sequences. All the sequences were derived from verified enzymatic activities of thermophilic or hyperthermophilic archaea unless stated otherwise. The sequences from *S. acidocaldarius* were analysed by BLASTP programme using the complete genome sequence (Chen *et al.*, unpublished; http//dac.molbio.ku.dk). All the assigned enzymatic functions for the proteins of *S. solfataricus* P2 were checked with the annotations in public protein databases, such as the BRaunschweig ENzyme DAtabase (BRENDA) [26], clusters of orthologous groups of proteins (COG) [27], InterPro [28] and the fee-based ERGO bioinformatics suite [29]. The reconstructed pathways were compared with the previous reports [9, 30, 31] and the Kyoto Encyclopaedia of Genes and Genomes (KEGG) [32].

3 Results and discussion

3.1 Generation and application of a 2-DE map

Figure 1 shows an image of the 2-DE reference map for *S. solfataricus*. With CBB G-250, approximately 500 spots were visualised. The highest spot count was obtained in the region pI = 5–9, and proteins ranged in size from 15 to 123 kDa (predicted values). In total, 255 spots were selected for MS analysis on the basis of their relative high abundance. In addition, faint spots were selected to test the sensitivity of the MS method. In total, 325 unique proteins in 255 spots were identified, with even the faintest spots yielding significant MOWSE scores (>51). All 255 spots were found on the triplicate gels. The complete dataset is presented in the supplementary material. A subset, representing key elements of central energy metabolism and other relevant proteins is discussed more extensively in this paper. The highest MOWSE score, 1362, was achieved for elongation factor 2 (Sso0728, spot 26). Generally, one peptide (intact mass and MS/MS ion spectrum) was sufficient for confident identification of a *S. solfataricus* protein against the full MSDB. In most cases, however, multiple peptides of the same protein were recovered from a spot. On average, the sequence coverage was 30%. The highest sequence coverage (75%) was found for the α-subunit of the proteasome (Sso0738) in spot 213. There was no correlation between the sequence coverage and the protein size. However, larger proteins usually resulted in higher MOWSE scores. This is due to the fact that larger proteins generate a larger number of unique peptides after tryptic digestion. For example, MOWSE scores greater than 800 were only obtained for proteins larger than 48 kDa.

The number of proteins that matched ORFs that are either hypothetical or conserved hypothetical proteins was 157 (48%). This is similar compared to the expected 53%, on the basis of the genome composition. This was also found in a similar study on the *Methanocaldococcus jannaschii* proteome [33]. Interestingly, there were only two hypothetical proteins amongst the 20 most intense spots (Sso0029, Sso0099 relating to spots 130 and 224 respectively). The relatively high abundance of those proteins suggests an important function.

Another important observation is that a number of proteins were found in more than one spot. Interestingly, this was true for a large number of proteins involved in the TCA cycle (*e.g.* 2-oxoacid:ferredoxin oxidoreductase (Sso2815) was found in eight different spots). There are a number of explanations for this: (i) isoforms or posttranslationally modified versions of the protein might be present in the cell, (ii) the protein was modified during protein extraction or during 2-DE (*e.g.* proteolysis, methionine oxidation), (iii) the protein does not resolve well on the gel and therefore "smears" out over a large pH or mass range or (iv) the denaturating conditions are not strong enough to completely break protein associations. The presence of a protein in multiple spots was

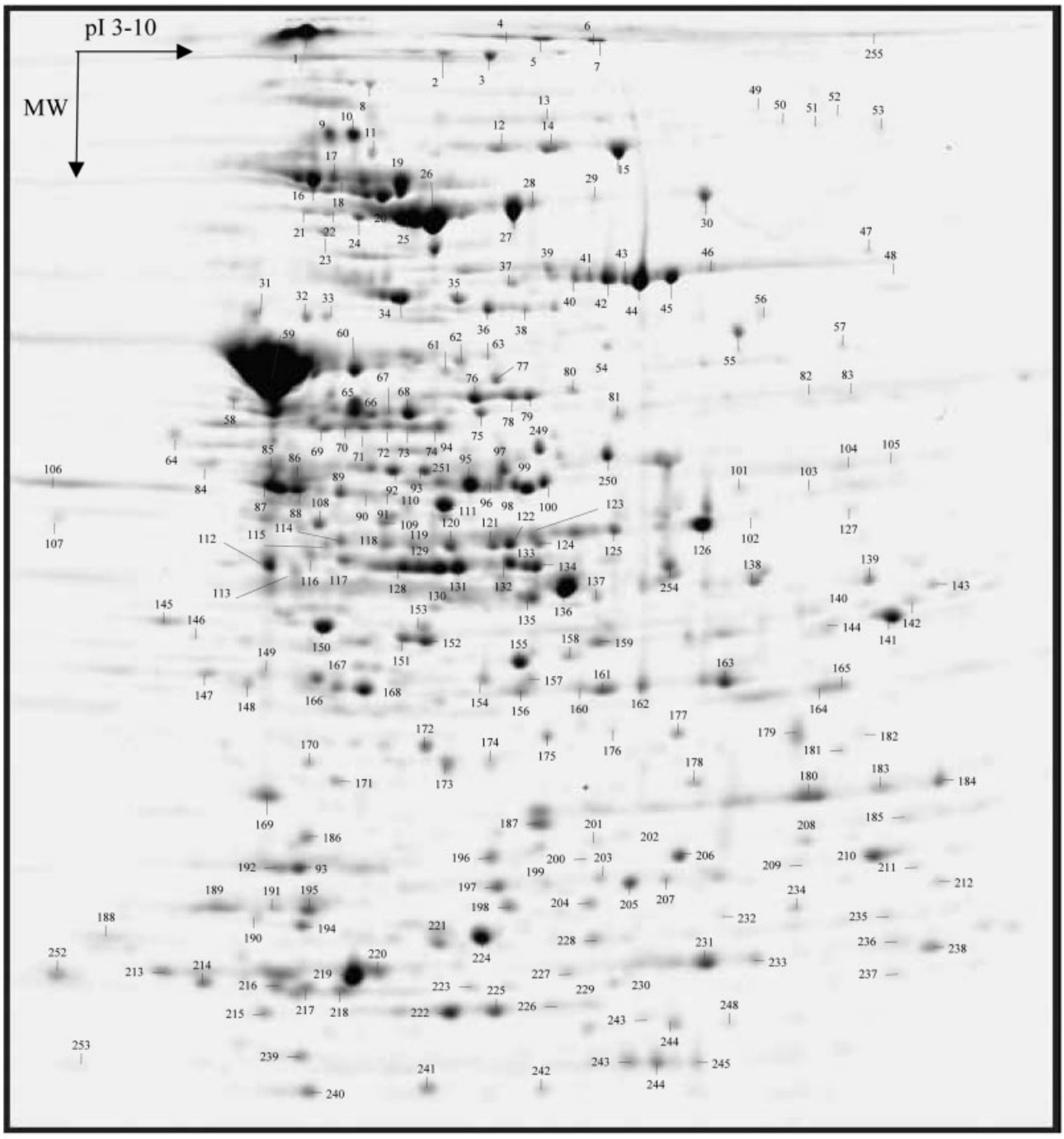

Figure 1. 2-DE reference map for *S. solfataricus* grown on glucose. All numbered spots were subjected to LC-MS-MS analysis. Results are displayed in Suppl. Table 1.

also observed in similar proteomic studies [33]. To find PTMs, all mass spectra were searched again but this time with phosphorylation of serine or threonine, and with methylation set as variable modifications. Unfortunately, no consistent results were obtained, and therefore more specific studies targeted to identify PTMs are necessary.

In a number of cases, multiple proteins *per* spot were found. Often these proteins have similar molecular weights (MW) and p*I*s indicating that the resolution on the gel was insufficient to resolve these proteins into single protein spots. In other cases however, proteins in the same spot differ significantly in MW and p*I*. These represent biologically

interesting cases since these could indicate stable protein associations. An example was found in spot 1, where subunits α, β and γ of aldehyde oxidoreductase (Sso2636, Sso2637, Sso2639) were found.

Protein quantitation was performed on the basis of ^{15}N metabolic labelling as recently described. With this method a number of problems associated with 2-DE (*e.g.* multiple proteins *per* spot) can be avoided. Moreover, the reproducibility of gel staining becomes of lesser importance since protein quantitation takes place on the MS [34].

Figure 2 shows an example of a TOF-MS spectrum containing both the light and the heavy versions of the peptide IFGSLSSNYVLTK. This peptide is derived from the KDG aldolase (Sso3197). The light peptide at *m/z* 714.99 corresponds to the yeast extract + tryptone (YT)-grown cells and the heavy peptide at *m/z* 722.47 corresponds to the glucose (G)-grown cells. The relative abundance of the heavy and light peptide can now be calculated by determining the ratio of the peak areas. Note that the difference in mass between the heavy and light versions of the peptide corresponded exactly to the number of nitrogen atoms in the peptide, in this case 15 atoms ($m/z = 7.5$). Table 1 summarises the differential proteomic data obtained in this way, as well as the corresponding transcriptomic data. In Section 3.3, these data are used for a discussion of the central carbon metabolism in *S. solfataricus*.

3.2 Exploration of the transcriptome

In total, 1581 of the 2315 genes printed on the microarray were used in the analysis (selected, according to criteria described in Section 2.8). There were 184 significant differentially expressed genes ($p < 0.05$; p is the statistical certainty that the observed change in ratio is *not* caused by a biological effect). In total, 135 and 49 genes are up-regulated under glucose and YT conditions respectively. Of these up-regulated genes 23 and 20% were annotated as either hypothetical or conserved hypothetical. Interestingly, these percentages are lower than the expected 53%.

Of the up-regulated genes, 16 and 10% were involved in amino acid metabolism under glucose and YT conditions respectively. Although knowledge about amino acid metabolism in *S. solfataricus* is limited, regulation in this functional group was expected since amino acids are expected to be synthesised under glucose conditions and predominantly degraded under YT conditions. These data, therefore, provide an excellent starting point for amino acid metabolism reconstruction. Future biochemical and proteomic studies are necessary to confirm the exact composition and direction of the responsible pathways.

Interestingly, three genes involved in nitrogen metabolism were regulated: (i) glutamate synthase (Sso0684; 0.15) (ii) glutamine synthase (Sso0366; 0.27) and (iii) glutamate dehydrogenase (Sso2044; 6.29), absolute ratios are given as YT/G. These results show that cells which grow on glucose assimilate nitrogen by the sequential action of glutamine synthase and glutamate synthase. Under YT conditions, glutamate dehydrogenase produces free ammonium by converting glutamate into 2-oxoglutarate. This is necessary because there is an excess of nitrogen bound to carbon when grown in the presence of YT.

Transport and binding proteins are also a major group of up-regulated genes (12 and 8% for glucose and YT respectively). Previously, it was shown that both glucose and YT-

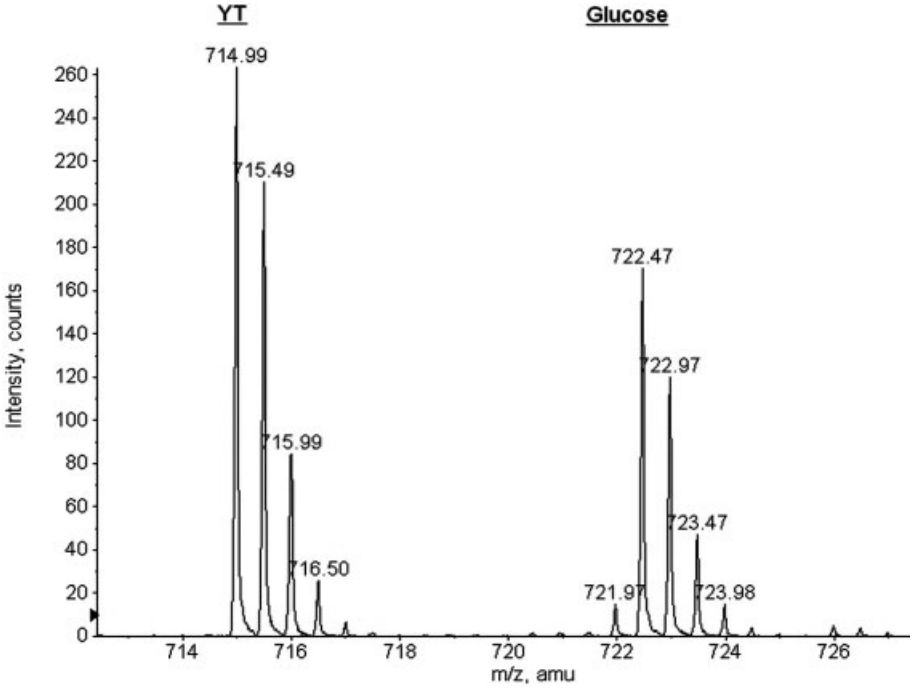

Figure 2. Peptide quantitation. TOF-MS spectrum of an ^{15}N labelled and an unlabelled peptide. Peak on the left at *m/z* 714.99 represents the unlabelled version of the peptide (protein from cells grown on yeast extract + tryptone (YT)). Peak at the right at *m/z* 7.22.47 represents the ^{15}N labelled version of the peptide (protein from cells grown on glucose). This peptide was identified as IFGSLSSNYVLTK, corresponding to KDG aldolase (Sso3197). Ratio between the areas of the heavy and light versions of this peptide was 1.56.

Table 1. Relative abundances of mRNA and protein levels of the genes involved in central metabolic pathways of *S. solfataricus* grown on yeast extract and tryptone (YT) compared to glucose (G)

Locus	Enzyme description	EC	COG	Trans-criptomics[a)]	Proteomics[a)]	Refe-rence
Glycolysis						
Sso3003	Glucose-1-dehydrogenase	1.1.1.47	1063	NS	NF	[16]
Sso2705	Gluconolactonase	3.1.1.17	3386	1.15 ± 0.07	NF	[9]
Sso3041	Gluconolactonase	3.1.1.17	3386	NF	NF	
Sso3198	Gluconate dehydratase	4.2.1.39	4948	1.00 ± 0.07	1.42 ± 0.14	[55, 56]
Sso3197	KDG aldolase	4.1.2.-	0329	0.96 ± 0.19	1.55 ± 0.05	[57]
Sso3195	KDG kinase	2.7.1.45	0524	1.19 ± 0.15	NF	[9]
Sso3194	GAP dehydrogenase (nonphosphorylating)	1.2.1.3	1012	0.87 ± 0.10	0.66 ± 0.07	[14, 58]
Sso2639[c)]	Aldehyde oxidoreductase, α-subunit	1.2.7.-	1529	0.65 ± 0.01[b)]	4.51 ± 0.78	[59]
Sso2636[c)]	Aldehyde oxidoreductase, β-subunit		1319	0.55 ± 0.13[b)]	4.89 ± 0.40	
Sso2637[c)]	Aldehyde oxidoreductase, γ-subunit		2080	0.62 ± 0.14[b)]	4.22 ± 1.03	
Sso0666	Glycerate kinase	2.7.1.-	2379	0.70 ± 0.24	NF	[9, 13]
Sso0981	PK	2.7.1.40	0469	0.98 ± 0.10	NF	[60]
Glycolysis/gluconeogenesis						
Sso0417	Phosphoglycerate mutase	5.4.2.1	3635	1.03 ± 0.13	1.55 ± 0.14	[61]
Sso2236	Phosphoglycerate mutase	5.4.2.1	0406	NS	NF	
Sso0913	Enolase	4.2.1.11	0148	1.36 ± 0.35	1.59 ± 0.23	[62]
Gluconeogenesis						
Sso0883	Phospho*enol*pyruvate synthase	2.7.9.2	0574	1.62 ± 0.08[b)]	1.77 ± 0.22	[63]
Sso0527	Phosphoglycerate kinase	2.7.2.3	0126	1.26 ± 0.26	2.30 ± 0.28	[64]
Sso0528	GAP dehydrogenase (phosphorylating)	1.2.1.12	0057	1.07 ± 0.20	1.16 ± 0.02	[52]
Sso2592	Triose-phosphate isomerase	5.3.1.1	0149	NF	1.17 ± 0.12	[65]
Sso3226	Fructose-bisphosphate aldolase	4.1.2.13	1830	NS	1.84 ± 0.10	[66]
Sso0286	Fructose-bisphosphatase	3.1.3.11	1980	1.24 ± 0.18	1.32 ± 0.05	[67]
Sso2281	Glucose-6-phosphate isomerase	5.3.1.9	0166	1.01 ± 0.13	1.51 ± 0.10	[68]
Sso0207	Phosphoglucomutase	5.4.2.2	1109	1.03 ± 0.32	1.55 ± 0.01	[69]
Tricarboxylic acid cycle						
Sso2589	Citrate synthase	2.3.3.1	0372	0.84 ± 0.09	1.02 ± 0.03	[70, 71]
Sso1095	Aconitase	4.2.1.3	1048	1.05 ± 0.14	1.11 ± 0.03	[45]
Sso2182	Isocitrate dehydrogenase	1.1.1.42	0538	1.34 ± 0.65	1.18 ± 0.03	[53]
Sso2815[d)]	2-oxoacid:ferredoxin oxidoreductase α/γ-subunit	1.2.7.1	0674	0.89 ± 0.07	0.56 ± 0.05	[49–51]
		1.2.7.3	1014			
Sso2816[d)]	2-oxoacid:ferredoxin oxidoreductase β-subunit		1013	0.85 ± 0.31	0.60 ± 0.02	
Sso2482	Succinate-CoA ligase, α-subunit	6.2.1.5	0074	0.93 ± 0.25	0.54 ± 0.04	[42]
Sso2483	Succinate-CoA ligase, β-subunit		0045	0.94 ± 0.30	0.51 ± 0.05	
Sso2356	Succinate dehydrogenase, subunit A	1.3.99.1	1053	NS	0.58 ± 0.4	[72]
Sso2357	Succinate dehydrogenase, subunit B		0479	0.75 ± 0.28	NF	
Sso2358	Succinate dehydrogenase, subunit C		2048	0.94 ± 0.27	NF	
Sso2359	Succinate dehydrogenase, subunit D			0.89 ± 0.16	NF	
Sso1077	Fumarate hydratase	4.2.1.2	0114	1.08 ± 0.10	1.53 ± 0.09	[73, 74]
Sso2585	Malate dehydrogenase	1.1.1.37	0039	0.82 ± 0.27	0.69 ± 0.01	[54]
Glyoxylate shunt						
Sso1333	Isocitrate lyase	4.1.3.1	2224	0.30 ± 0.07[b)]	NF	[46]
Sso1334	Malate synthase	2.3.3.9	2225	1.11 ± 0.47	1.18 ± 0.04	
C3/C4 interconversions						
Sso2869	Malic enzyme	1.1.1.38	0281	1.05 ± 0.24	1.92 ± 0.15	[47]
Sso2537	Phosphoenolpyruvate carboxykinase	4.1.1.32	1274	1.42 ± 0.42	NF	[48]
Sso2256	Phosphoenolpyruvate carboxylase	4.1.1.31	1892	0.83 ± 0.18	0.88 ± 0.17	[43, 44]

NF: not found, NS: no significant signal.

a) Relative abundance ratio with SD yeast extract + tryptone-grown cells/glucose-grown cells (YT/G).

b) Probability value (*p*) smaller than 0.05.

c) Enzyme complex has broad substrate specificity for aldehydes.

d) Exhibits pyruvate, 2-oxoglutarate and 2-oxobutyrate oxidoreductase activity.

grown cells have the capacity to transport glucose [35]. This is reflected by the fact that the genes involved in glucose transport were not differentially expressed (Sso2847, Sso2848, Sso2849 and Sso2850). In addition, genes involved in dipeptide transport were up-regulated under YT conditions (Sso1282; 2.01/Sso2615; 1.74/Sso2616; 1.57). Interestingly, genes involved in maltose transport were slightly up-regulated under glucose conditions (Sso3053; 0.36/Sso3058; 0.50/Sso3059; 0.53).

3.3 Metabolic pathway reconstruction

During the last two decades, the main metabolic pathways in *Sulfolobus* spp. have been the subject of extensive experimental research. This has led to a profound understanding of the enzymes and protein complexes that are involved in the glycolysis, the TCA and related metabolic conversions [9, 36]. The availability of the genome sequences of *S. solfataricus* [2], *S. tokodaii* [37] and *S. acidocaldarius* (Chen *et al.*, unpublished work; http//dac.molbio.ku.dk) has recently allowed for the identification of the genes encoding these proteins by matching full length or N-terminal protein sequences to the predicted proteomes. A reconstruction of the central carbon metabolic pathways in *S. solfataricus* was performed (Fig. 3). The results should be taken with a degree of caution, since significant differences exist in the physiology between the three *Sulfolobus* species [12]. Almost all proteins involved in this scheme have been experimentally verified in either *Sulfolobus* spp. or other hyperthermophilic Archaea, such as *Thermoproteus tenax, Archaeoglobus fulgidus, Thermoplasma acidophilum, P. furiosus, Thermococcus kodakaraensis, Methanothermus fervidus* and *M. jannaschii*. Moreover, the vast majority of the anticipated proteins in *S. solfataricus* were found on the 2-DE reference map (Fig. 2). On average, the TCA cycle proteins made up approximately 12% of the total staining intensity.

3.4 Glycolysis and gluconeogenesis

The genus *Sulfolobus* is known to degrade glucose according to a modified version of the ED pathway. While in most cases phosphorylation in the bacterial ED pathway occurs at the level of glucose, gluconate or KDG, *S. solfataricus* has been reported to utilise a nonphosphorylated version of the ED pathway, which phosphorylates only at the level of glycerate [13, 38]. Recent experimental findings, however, indicated the presence of a semiphosphorylated ED pathway, in which KDG is phosphorylated and subsequently cleaved forming pyruvate and glyceraldehyde-3-phosphate (GAP) by the action of the KDG kinase (Sso3195) and the KDG aldolase (Sso3197) respectively. GAP is then oxidised by a nonphosphorylating GAP dehydrogenase (GAPN, Sso3194) forming 3-phosphoglycerate (3PG) [14]. The only net difference between the non- and semiphosphorylated pathways is the fact that either reduced ferredoxin (Fd_R) or NADPH is produced, since neither pathway directly yields ATP by substrate level phosphorylation.

The intrinsic irreversibility of several ED enzymes, such as the gluconate dehydratase, the aldehyde oxidoreductase and GAPN, prevents the ED to operate in the gluconeogenic direction, which is, for instance, required to store energy in the form of glycogen [39]. Another important role for the gluconeogenic EMP pathway is the production of fructose-6-phosphate (F6P), which has been proposed to be the main precursor for the pentose phosphate pathway (PPP) [9]. Except for three kinases (GK glucokinase, PFK phosphofructokinase and PK), the catabolic EMP pathway consists of reversible enzymes. Although the genes encoding a GK and PFK were absent, the genes encoding the reversible EMP enzymes were all found in the genome of *Sulfolobus*. Moreover, a gene encoding a fructose-1,6-bisphosphatase (FBPase) was also detected. Because it is known that the catabolic EMP pathway is not operational in *Sulfolobus* [38], it is likely that these EMP enzymes serve a gluconeogenic role. The simultaneous operation of both the ED and a gluconeogenic EMP pathway, however, requires a strict control of the metabolic flux through the pathway in order to prevent an energetically futile cycle. Allosteric regulation, posttranslational protein modification and regulation at the transcriptional level are common strategies to modulate the activity and abundance of key enzymes, such as the FBPase.

Although glycolysis in *Sulfolobus* is well studied, there are still unconfirmed genes and activities in the pathway. For instance, the transcriptome analysis revealed the expression of one of two putative gluconolactonases (Sso2705) that have generally been omitted in the analysis of the ED pathway, since the reaction from gluconolactone to gluconate also occurs spontaneously [40]. The expression of the enzyme, however, would suggest a functional role in the metabolism of *Sulfolobus*. Additionally, only one of two phosphoglycerate mutases (Sso0417) that were found in its genome was expressed in both the proteome and transcriptome, while the other type (Sso2236) remained undetected. Expression of the predicted glycerate kinase (Sso0666) was only detected at the mRNA level.

3.5 TCA

Sulfolobus spp. is an obligate aerobe that primarily obtains energy by the oxidation of organic molecules and elemental sulphur [41]. This oxidation results in the formation of reduced electron carriers, such as NAD(P)H, Fd_R and $FADH_2$. The majority of these reducing equivalents are generated in the TCA cycle. *Per* round of the cycle, the succinate-CoA ligase of *Sulfolobus* generates one molecule of ATP, instead of the commonly produced GTP [42]. Apart from being the main metabolic converter of chemical energy, the TCA cycle intermediates serve an important role as biosynthetic precursors for many cellular components, such as amino acids. Consequently, when too many intermediates are withdrawn from the cycle, they need to be replenished by anaplerotic enzyme reactions. The phospho*enol*pyruvate carboxylase (PEPC), which forms oxaloacetate

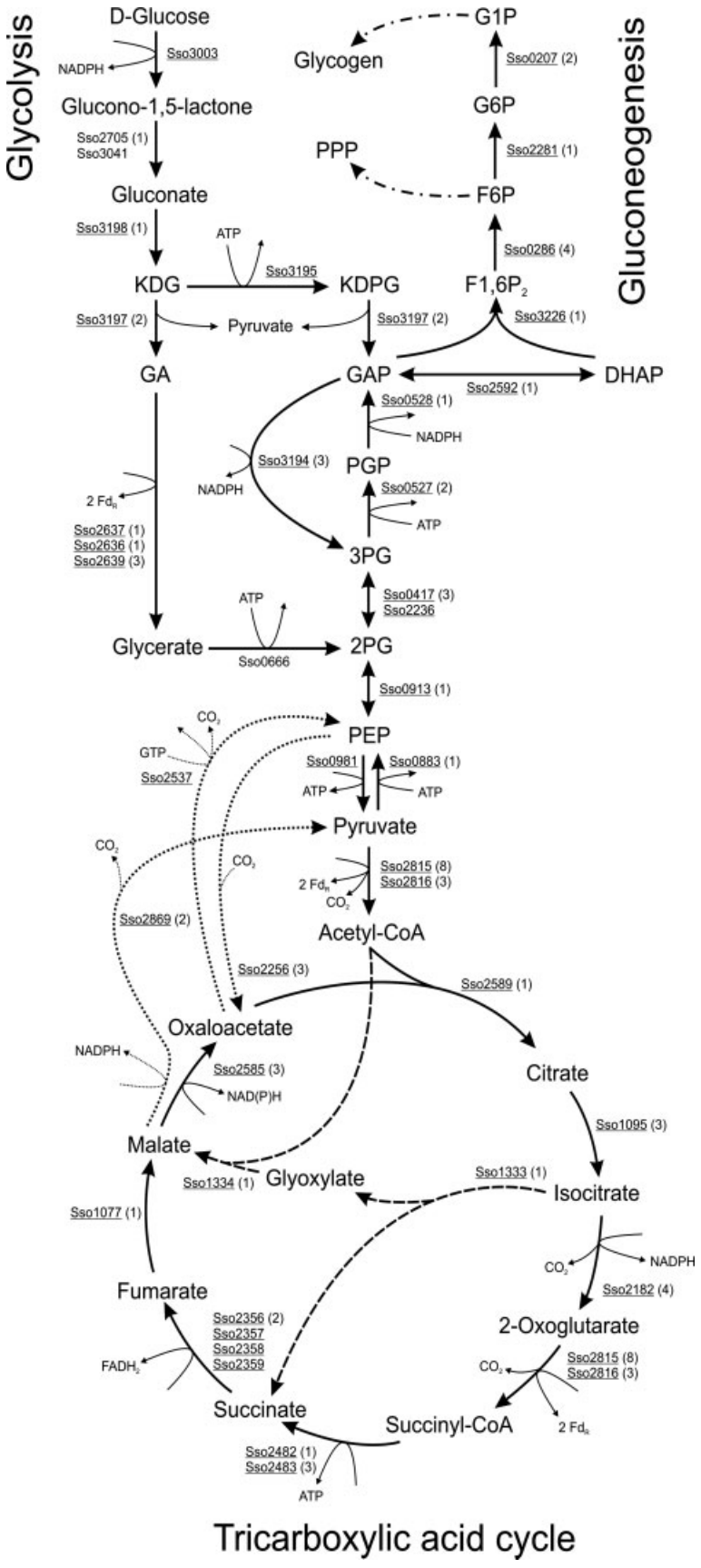

Figure 3. Reconstruction of the central metabolic pathways in *S. solfataricus*. Genes involved in the glycolysis, gluconeogenesis and citric acid cycle were surveyed and are indicated by their locus name. Underlined genes were experimentally verified in *Sulfolobus* or related hyperthermophilic Archaea (Table 1). Number of spots that were found on the 2-DE reference map is indicated between brackets. Glyoxylate shunt in shown by dashed arrows, while the three-to-four-carbon interconversions are depicted by dotted arrows. Mixed dashed and dotted arrows indicate that the exact pathway to glycogen and pentoses is unknown. Following abbreviations were used: KD(P)G, 2-keto-3-deoxy-d-gluconate-(6-phosphate); GA(P), glyceraldehyde-(3-phosphate); PGP, 1,3-bisphosphoglycerate; 3PG, 3-phosphoglycerate; 2PG, 2-phosphoglycerate; PEP, phospho*enol*pyruvate; DHAP, dihydroxyacetonephosphate; $F1,6P_2$, fructose-1,6-bisphosphate; F6P, fructose-6-phosphate; G6P, glucose-6-phosphate; G1P, glucose-1-phosphate; Fd_R, reduced ferredoxin; PPP, pentose phosphate pathway. NAD(P)H indicates that both NAD^+ and $NADP^+$ can be used as a cofactor. Arrows represent the presumed physiologically relevant direction of catalysis and are not indicative of enzymatic reversibility.

from phospho*e-nol*pyruvate, is the only anaplerotic enzyme from *Sulfolobus*, which has been described to date [43, 44]. A gene product with high similarity to known pyruvate carboxylases could not be detected in the predicted proteome of *Sulfolobus*. In the glyoxylate shunt, which is normally only active during growth on acetate, isocitrate and acetyl-CoA are converted into succinate and malate by the action of the isocitrate lyase and the malate synthase. Interestingly, the isocitrate lyase of glucose-grown *S. acidocaldarius* cells copurified with the aconitase [45, 46]. Not only would this suggest a cytosolic association of the enzymes, but it also suggests that the glyoxylate shunt operates under saccharolytic conditions. This pathway may therefore constitute another way of replenishing four-carbon TCA cycle intermediates.

When there is an excess of TCA intermediates, for instance during growth on proteinaceous substrates, both malate and oxaloacetate can be decarboxylated to pyruvate by the malic enzyme [47]. Oxaloacetate can also be converted to phospho*enol*pyruvate by the GTP-dependent carboxykinase [48]. These four-to-three carbon conversions then provide the precursors that are required in, for instance, the gluconeogenesis pathway. In contrast to aerobic bacteria and eukaryotes, *Sulfolobus* uses ferredoxin instead of NAD^+ as a cofactor in the formation of acetyl-CoA from pyruvate and succinyl-CoA from 2-oxoglutarate [49]. The protein complex responsible for both conversions was shown to consist of two subunits: a fused α/γ subunit (Sso2815) and a β subunit (Sso2816) [50, 51]. The genome sequences of the three *Sulfolobus* species, however, revealed several paralogues of ferredoxin-dependent 2-oxoacid oxidoreductases, which might also be involved in these conversions.

What is also evident from this reconstruction is that almost all dehydrogenases in the central carbon metabolism of *Sulfolobus* show a clear cofactor preference for $NADP^+$ over NAD^+ [2, 16, 42, 47, 52, 53]. The only exception to this rule seems to be the malate dehydrogenase, which, at least *in vitro*, uses both electron acceptors equally well [54]. In bacteria and eukaryotes, most NADPH is usually formed in the PPP and used for reductive biosynthesis purposes. In *Sulfolobus*, the apparent enzyme preference for $NADP^+$ would suggest a more general role of its reduced form, in energy conservation by oxidative phosphorylation. Interestingly, as noted by She *et al.* [2] all genes encoding the NAD(P)H dehydrogenase complex are present in the genome, except the three that encode the subunits which are required for NAD(P)H binding and oxidation. It has been proposed that the reducing equivalents are first transferred to ferredoxin by an NADPH:ferredoxin oxidoreductase, before entering the respiratory chain [2].

3.6 Regulation of the main metabolic pathways

Insight was obtained into the regulation of the genes anticipated in glycolysis, gluconeogenesis and TCA cycle by measuring the relative abundance of their mRNA and protein levels by using a whole-genome DNA microarray and a quantitative proteomics approach respectively (Table 1). In the measurements, 35 out of 41 transcript ratios were determined, while 29 out of 41 protein ratios were analysed on 2-DE gels. On average the proteomic and transcriptomic data correlate reasonably well. For 26 genes, both proteomic data and transcriptomic data are presented. In general, changes at proteomic and transcriptomic level show a similar trend, however, proteomic changes tend to be more pronounced. In only three cases the proteomic data contradict the transcriptome data. This concerns the three subunits for aldehyde dehydrogenase (Sso2639, Sso2636 and Sso2637). However, the fact that these clustered genes show a similar ratio at proteomic or transcriptomic level indicates the consistency of the data. Interestingly, all three subunits were found in the same protein spot on the gel, suggesting that a strong (non-covalent) interaction exists between them. The stability of the protein complex might be affected by stabilising factors such as cofactors that may lead to different degrees of aggregation under different growth conditions. In terms of regulatory effects, the GAPN was up-regulated under glucose conditions, or alternatively, down-regulated during growth in YT media. This is not surprising, since GAP is the crucial intermediate between the ED and gluconeogenic EMP, and too much of the strictly catabolic GAPN would be likely to interfere with gluconeogenesis. The enzymes involved in gluconeogenesis were all slightly up-regulated during growth on YT media, in agreement with expectations. Especially the phospho*enol*pyruvate synthase and the phosphoglycerate kinase, key enzymes of the pathway, appeared to be most differentially expressed.

The expression levels of the TCA-cycle genes were only marginally different under the two conditions. Under glucose conditions, several enzymes of the TCA cycle were slightly induced at proteomic level, including the 2-oxoacid:ferredoxin oxidoreductase, the succinate-CoA ligase, the succinate dehydrogenase and the malate dehydrogenase. This was also true for some enzymes that replenish the four-carbon TCA cycle intermediates, such as the isocitrate lyase and the PEPC. This ensures that sufficient oxaloacetate is present to serve as biosynthetic precursor and as an acceptor molecule for acetyl-CoA. The differences may be due to the fact that glucose catabolism mainly results in acetyl-CoA and oxaloacetate formation, whereas peptide degradation probably yields various central intermediates of carbon metabolism, such as pyruvate (Ala, Cys, Trp, Thr, Ser, Gly), acetyl-CoA (Phe, Tyr, Ile, Leu, Lys, Trp, Thr), 2-oxoglutarate (Arg, Gln, His, Pro, Glu), succinyl-CoA (Ile, Met, Val, Thr), fumarate (Phe, Tyr, Asp) and oxaloacetate (Asn, Asp).

4 Concluding remarks

In this study, we have created a proteome reference map for *S. solfataricus* consisting of 325 proteins in 255 spots, and have reconstructed its central carbon metabolic pathways. The expression of the genes in these pathways was analysed

by measuring the relative abundance of mRNA and protein under peptide- or sugar-degrading conditions. Surprisingly, most observed differences were small. Despite this, the expression of some key enzymes in glycolysis, gluconeogenesis and TCA cycle were significantly altered. Apart from looking at abundance levels, proteomics studies that focus on the modulation of enzyme activity by protein PTM are now ongoing. These studies will provide additional clues that will reveal the details of regulation of the central carbon metabolism in *S. solfataricus*.

The authors wish to thank Anders Andersson and Peter Nilsson (Department of Biotechnology, Royal Institute of Technology, Stockholm, Sweden); Magnus Lundgren and Rolf Bernander (Department of Molecular Evolution, Evolutionary Biology Center, Uppsala University, Uppsala, Sweden) for supplying the microarray, technical assistance and advice. We thank the University of Sheffield and UK's SRIF Infrastructure funds for support. A.P.L.S. thanks the University of Sheffield and the EPSRC for a scholarship. M.G.J.V. thanks the European Union's ERASMUS Programme. P.C.W. thanks the UK's Engineering and Physical Sciences Research Council (EPSRC) for provision of an Advanced Research Fellowship (GR/A11311/01). This work was partly supported by a grant from the European Union in the framework of the SCREEN project (contract QLK3-CT-2000-00649).

5 References

[1] Zillig, W., Stetter, K. O., Wunderl, S., Schulz, W., Priess, H. *et al.*, *Arch. Microbiol.* 1980, *125*, 259–269.

[2] She, Q., Singh, R. K., Confalonieri, F., Zivanovic, Y., Allard, G. *et al.*, *Proc. Natl. Acad. Sci. USA* 2001, *98*, 7835–7840.

[3] Peterson, J. D., Umayam, L. A., Dickinson, T., Hickey, E. K., White, O., *Nucleic Acids Res.* 2001, *29*, 123–125.

[4] Cannio, R., Contursi, P., Rossi, M., Bartolucci, S., *Extremophiles* 2001, *5*, 153–159.

[5] Stedman, K. M., Schleper, C., Rumpf, E., Zillig, W., *Genetics* 1999, *152*, 1397–1405.

[6] Worthington, P., Hoang, V., Perez-Pomares, F., Blum, P., *J. Bacteriol.* 2003, *185*, 482–488.

[7] Jonuscheit, M., Martusewitsch, E., Stedman, K. M., Schleper, C., *Mol. Microbiol.* 2003, *48*, 1241–1252.

[8] Contursi, P., Cannio, R., Prato, S., Fiorentino, G., Rossi, M. *et al.*, *FEMS Microbiol. Lett.* 2003, *218*, 115–120.

[9] Verhees, C. H., Kengen, S. W., Tuininga, J. E., Schut, G. J., Adams, M. W. *et al.*, *Biochem. J.* 2003, *375*, 231–246.

[10] Adams, M. W. W., Holden, J. F., Menon, A. L., Schut, G. J., Grunden, A. M. *et al.*, *J. Bacteriol.* 2001, *183*, 716–724.

[11] Schonheit, P., Schafer, T., *World J. Microbiol. Biotechnol.* 1995, *11*, 26–57.

[12] Schafer, G., *Biochim. Biophys. Acta* 1996, *1277*, 163–200.

[13] De Rosa, M., Gambacorta, A., Nicolaus, B., Giardina, P., Poerio, E. *et al.*, *Biochem. J.* 1984, *224*, 407–414.

[14] Ahmed, H., Ettema, T. J. G., Tjaden, B., Geerling, A. C. M., van der Oost, J. *et al.*, *Biochem. J.* 2005, *390*, 529–540.

[15] Lamble, H. J., Heyer, N. I., Bull, S. D., Hough, D. W., Danson, M. J., *J. Biol. Chem.* 2003, *278*, 34066–34072.

[16] Lamble, H. J., Heyer, N. I., Bull, S. D., Hough, D. W., Danson, M. J., *J. Biol. Chem.* 2003, *278*, 34066–34072.

[17] Schut, G. J., Brehm, S. D., Datta, S., Adams, M. W., *J. Bacteriol.* 2003, *185*, 3935–3947.

[18] Zaigler, A., Schuster, S. C., Soppa, J., *Mol. Microbiol.* 2003, *48*, 1089–1105.

[19] Snijders, A. P., de Vos, M. G., Wright, P. C., *J. Proteome Res.* 2005, *4*, 578–585.

[20] Pappin, D. J., Hojrup, P., Bleasby, A. J., *Curr. Biol.* 1993, *3*, 327–332.

[21] Brinkman, A. B., Bell, S. D., Lebbink, R. J., de Vos, W. M., van der Oost, J., *J. Biol. Chem.* 2002, *277*, 29537–29549.

[22] Lundgren, M., Andersson, A., Chen, L., Nilsson, P., Bernander, R., *Proc. Natl. Acad. Sci. USA* 2004, *101*, 7046–7051.

[23] Andersson, A., Bernander, R., Nilsson, P., *Bioinformatics* 2005, *21*, 325–332.

[24] Tusher, V. G., Tibshirani, R., Chu, G., *Proc. Natl. Acad. Sci. USA* 2001, *98*, 5116–5121.

[25] Altschul, S. F., Madden, T. L., Schaffer, A. A., Zhang, J., Zhang, Z. *et al.*, *Nucleic Acids Res.* 1997, *25*, 3389–3402.

[26] Schomburg, I., Chang, A., Ebeling, C., Gremse, M., Heldt, C. *et al.*, *Nucleic Acids Res.* 2004, *32*, D431–D433.

[27] Tatusov, R. L., Fedorova, N. D., Jackson, J. D., Jacobs, A. R., Kiryutin, B. *et al.*, *BMC Bioinformatics* 2003, *4: 41*.

[28] Mulder, N. J., Apweiler, R., Attwood, T. K., Bairoch, A., Bateman, A. *et al.*, *Nucleic Acids Res.* 2005, *33*, D201–D205.

[29] Overbeek, R., Larsen, N., Walunas, T., D'Souza, M., Pusch, G. *et al.*, *Nucleic Acids Res.* 2003, *31*, 164–171.

[30] Huynen, M. A., Dandekar, T., Bork, P., *Trends Microbiol.* 1999, *7*, 281–291.

[31] Ronimus, R. S., Morgan, H. W., *Archaea* 2003, *1*, 199–221.

[32] Kanehisa, M., Goto, S., Kawashima, S., Okuno, Y., Hattori, M., *Nucleic Acids Res.* 2004, *32*, D277–D280.

[33] Giometti, C. S., Reich, C., Tollaksen, S., Babnigg, G., Lim, H. *et al.*, *J. Chromatogr. B Analyt. Technol. Biomed. Life Sci.* 2002, *782*, 227–243.

[34] Snijders, A. P. L., de Vos, M. G., Koning, B., Wright, P. C., *Electrophoresis* 2005, *26*, 3191–3199.

[35] Elferink, M. G., Albers, S. V., Konings, W. N., Driessen, A. J., *Mol. Microbiol.* 2001, *39*, 1494–1503.

[36] Danson, M. J., *Adv. Microb. Physiol.* 1988, *29*, 165–231.

[37] Kawarabayasi, Y., Hino, Y., Horikawa, H., Jin-no, K., Takahashi, M. *et al.*, *DNA Res.* 2001, *8*, 123–140.

[38] Selig, M., Xavier, K. B., Santos, H., Schonheit, P., *Arch. Microbiol.* 1997, *167*, 217–232.

[39] Skorko, R., Osipiuk, J., Stetter, K. O., *J. Bacteriol.* 1989, *171*, 5162–5164.

[40] Satory, M., Furlinger, M., Haltrich, D., Kulbe, K. B., Pittner, F. *et al.*, *Biotechnol. Lett.* 1997, *19*, 1205–1208.

[41] Brock, T. D., Brock, K. M., Belly, R. T., Weiss, R. L., *Arch. Microbiol.* 1972, *84*, 54–68.

[42] Danson, M. J., Black, S. C., Woodland, D. L., Wood, P. A., *FEBS* 1985, *179*, 120–124.

[43] Sako, Y., Takai, K., Uchida, A., Ishida, Y., *FEBS Lett.* 1996, *392*, 148–152.

[44] Ettema, T. J., Makarova, K. S., Jellema, G. L., Gierman, H. J., Koonin, E. V. *et al., J. Bacteriol.* 2004, *186*, 7754–7762.

[45] Uhrigshardt, H., Walden, M., John, H., Anemuller, S., *Eur. J. Biochem.* 2001, *268*, 1760–1771.

[46] Uhrigshardt, H., Walden, M., John, H., Petersen, A., Anemuller, S., *FEBS Lett.* 2002, *513*, 223–229.

[47] Bartolucci, S., Rella, R., Guagliardi, A., Raia, C. A., Gambacorta, A. *et al., J. Biol. Chem.* 1987, *262*, 7725–7731.

[48] Fukuda, W., Fukui, T., Atomi, H., Imanaka, T., *J. Bacteriol.* 2004, *186*, 4620–4627.

[49] Kerscher, L., Nowitzki, S., Oesterhelt, D., *Eur. J. Biochem.* 1982, *128*, 223–230.

[50] Zhang, Q., Iwasaki, T., Wakagi, T., Oshima, T., *J. Biochem. (Tokyo)* 1996, *120*, 587–599.

[51] Fukuda, E., Wakagi, T., *Biochim. Biophys Acta* 2002, *1597*, 74–80.

[52] Russo, A. D., Rullo, R., Masullo, M., Ianniciello, G., Arcari, P. *et al., Biochem. Mol. Biol. Int.* 1995, *36*, 123–135.

[53] Camacho, M. L., Brown, R. A., Bonete, M. J., Danson, M. J., Hough, D. W., *FEMS Microbiol Lett.* 1995, *134*, 85–90.

[54] Hartl, T., Grossebuter, W., Gorisch, H., Stezowski, J. J., *Biol. Chem. Hoppe Seyler* 1987, *368*, 259–267.

[55] Kim, S., Lee, S. B., *Biochem. J.* 2005, *387*, 271–280.

[56] Lamble, H. J., Milburn, C. C., Taylor, G. L., Hough, D. W., Danson, M. J., *FEBS Lett.* 2004, *576*, 133–136.

[57] Buchanan, C. L., Connaris, H., Danson, M. J., Reeve, C. D., Hough, D. W., *Biochem. J.* 1999, *343*, 563–570.

[58] Brunner, N. A., Brinkmann, H., Siebers, B., Hensel, R., *J. Biol. Chem.* 1998, *273*, 6149–6156.

[59] Kardinahl, S., Schmidt, C. L., Hansen, T., Anemuller, S., Petersen, A. *et al., Eur. J. Biochem.* 1999, *260*, 540–548.

[60] Schramm, A., Siebers, B., Tjaden, B., Brinkmann, H., Hensel, R., *J. Bacteriol.* 2000, *182*, 2001–2009.

[61] van der Oost, J., Huynen, M. A., Verhees, C. H., *FEMS Microbiol. Lett.* 2002, *212*, 111–120.

[62] Peak, M. J., Peak, J. G., Stevens, F. J., Blamey, J., Mai, X. *et al., Arch. Biochem. Biophys.* 1994, *313*, 280–286.

[63] Hutchins, A. M., Holden, J. F., Adams, M. W., *J. Bacteriol.* 2001, *183*, 709–715.

[64] Hess, D., Kruger, K., Knappik, A., Palm, P., Hensel, R., *Eur. J. Biochem.* 1995, *233*, 227–237.

[65] Kohlhoff, M., Dahm, A., Hensel, R., *FEBS Lett.* 1996, *383*, 245–250.

[66] Siebers, B., Brinkmann, H., Dorr, C., Tjaden, B., Lilie, H. *et al., J. Biol. Chem.* 2001, *276*, 28710–28718.

[67] Nishimasu, H., Fushinobu, S., Shoun, H., Wakagi, T., *Structure (Camb)* 2004, *12*, 949–959.

[68] Hansen, T., Wendorff, D., Schonheit, P., *J. Biol. Chem.* 2004, *279*, 2262–2272.

[69] Solow, B., Bischoff, K. M., Zylka, M. J., Kennelly, P. J., *Protein Sci.* 1998, *7*, 105–111.

[70] Smith, L. D., Stevenson, K. J., Hough, D. W., Danson, M. J., *FEBS Lett.* 1987, *225*, 277–281.

[71] Lohlein-Werhahn, G., Goepfert, P., Eggerer, H., *Biol. Chem. Hoppe Seyler* 1988, *369*, 109–113.

[72] Janssen, S., Schafer, G., Anemuller, S., Moll, R., *J. Bacteriol.* 1997, *179*, 5560–5569.

[73] Puchegger, S., Redl, B., Stoffler, G., *J. Gen. Microbiol.* 1990, *136*, 1537–1541.

[74] Colombo, S., Grisa, M., Tortora, P., Vanoni, M., *FEBS Lett.* 1994, *337*, 93–98.

